



Published in final edited form as:

Invest Radiol. 2010 January ; 45(1): 36–41. doi:10.1097/RLI.0b013e3181beada7.

Minimization of MR Contrast Weightings for the Comprehensive Evaluation of Carotid Atherosclerotic Disease

Xihai Zhao, MD, PhD^{*}, Hunter R. Underhill, MD^{*}, Chun Yuan, PhD^{*}, Minako Oikawa, MD, PhD^{*}, Li Dong, MD^{*}, Hideki Ota, MD, PhD^{*}, Thomas S. Hatsukami, MD[†], Qingjun Wang, MD[‡], Lin Ma, MD, PhD[‡], and Jianming Cai, MD, PhD[‡]

^{*}Department of Radiology, University of Washington, Seattle, WA

[†]Department of Surgery, University of Washington, Seattle, WA

[‡]Department of Radiology, Chinese People's Liberation Army General Hospital, Beijing, People's Republic of China

Abstract

Objective—Multicontrast, high-resolution carotid magnetic resonance imaging (MRI) has been validated with histology to quantify atherosclerotic plaque morphology and composition. For evaluating the lipid-rich necrotic core (LRNC) and fibrous cap, both of which are key elements in determining plaque stability, the combined pre- and postcontrast T1-weighted (T1W) sequences have been recently shown to have a higher reproducibility than other contrast weightings. In this study, we sought to determine whether contrast weightings beyond T1W (pre- and postcontrast) are necessary for comprehensive, quantitative, carotid plaque interpretation.

Materials and Methods—Our HIPAA compliant study protocol was approved by the IRB and all participants gave written, informed consent. Sixty-five participants with carotid stenosis >50% detected by ultrasound underwent carotid MRI with a standard multicontrast protocol (time-of-flight [TOF], T1W, contrast-enhanced [CE]-T1W, proton density [PD], and T2W). For each subject, images were partitioned into 3 combinations of contrast weightings (CW): (1) 2CW: T1W and CE-T1W; (2) 3CW: T1W, CE-T1W, and TOF; and (3) 5CW: T1W, CE-T1W, TOF, PD, and T2W. Each CW set was interpreted by 2 reviewers, blinded to results of each of the other CW combinations, via consensus opinion. Wall, lumen, and total vessel volumes, along with mean wall thickness were recorded. The presence or absence of calcification, LRNC, intraplaque hemorrhage (IPH), and surface disruption was also documented.

Results—Compared with 5CW, there was strong agreement in the parameters of plaque morphology for 2CW (intraclass correlation coefficient, 0.96–0.99) and 3CW (intraclass correlation coefficient, 0.97–1.00). Agreement with 5CW for the detection of plaque composition was stronger for 3CW compared with 2CW: Cohen's kappa, 0.59 versus 0.42 for calcification; 0.75 versus 0.47 for LRNC; 0.91 versus 0.88 for IPH; and 0.74 versus 0.34 for surface disruption. Using 5CW as the reference standard during receive-operating-characteristics analysis, 3CW compared with 2CW showed a larger area-under-the-curve for classifying the presence or absence

of calcification (0.78 vs. 0.69), LRNC (0.98 vs. 0.69), and surface disruption (0.87 vs. 0.65), and similar area-under-the-curve in classifying IPH (0.96 vs. 0.94).

Conclusion—Comprehensive, quantitative carotid plaque interpretation can be performed with T1W, CE-T1W, and TOF sequences. Elimination of PD and T2W sequences from the carotid MRI protocol may result in a substantial reduction in scan time. The ability to perform plaque interpretation on images acquired within a clinically acceptable scan time may broaden the research utility of carotid MRI and increase translatability to clinical applications.

Keywords

atherosclerosis; carotid artery; magnetic resonance imaging

Multicontrast magnetic resonance imaging (MRI) has been validated with histology to noninvasively characterize and quantify *in vivo* atherosclerotic disease in the carotid artery.^{1–6} Quantification of plaque morphology has been accomplished through black-blood sequences (T1-weighted [T1W]⁷ or proton density [PD])⁸ with adequate blood flow suppression that permits the differentiation of both the lumen and outer wall boundaries.^{9,10} Identification of plaque features has been enabled by combining the signals from different contrast weightings. The lipid-rich necrotic core (LRNC) manifests as a hypointense signal on T2W images and isointense on T1W.^{3,4} Intraplaque hemorrhage (IPH) has been characterized as a hyperintense signal on time-of-flight (TOF) and T1W,^{11,12} with a variable appearance on T2W and PD.^{11,13,14} Fibrous cap status (thick, thin, or ruptured) has been assessed with TOF and T2W.^{15–17} Finally, calcification has been detectable by a hypointense signal across all contrast weightings (TOF, T1W, PD, T2W).³ Recently, a gadolinium contrast-enhanced T1W (CE-T1W) sequence coupled with a precontrast T1W sequence has been demonstrated to discriminate the fibrous cap from the LRNC with stronger signal-to-noise ratio and better contrast-to-noise ratio than that of the T2W sequence.¹⁸ In addition, the utilization of gadolinium-based contrast agents has improved the quantification and reproducibility of the LRNC.^{19,20}

Although utilization of all contrast weightings (TOF, T1W, CE-T1W, PD, and T2W) has been advocated,²¹ each contrast weighting requires additional scan time. Beyond the associated increase in expense, longer scan times may lower overall image quality because of patient movement. Because T1W and/or CE-T1W sequences are integral for identifying each plaque feature, we hypothesized that T1W and CE-T1W sequences may be sufficient to fully characterize carotid atherosclerotic disease. The aim of this study was to determine whether contrast weightings beyond T1W (pre- and postcontrast) are necessary for comprehensive, quantitative, carotid plaque interpretation. The identification of the minimum number of contrast weightings necessary for the analysis of carotid atherosclerotic disease will help establish a reliable and cost-effective imaging protocol that may broaden the research and clinical utility of carotid MRI.

MATERIALS AND METHODS

Study Sample

Patients with carotid atherosclerotic disease were recruited for study enrollment using the following criteria: (1) neurologically asymptomatic and stenosis >50% in at least 1 carotid artery by duplex ultrasound; or (2) clinical history of a recent (<3 months) neurologic event (eg, amaurosis fugax, transient ischemic attack, or stroke) and stenosis >50% by duplex ultrasound in the symptomatic artery. The artery selected for carotid MR imaging, termed the index artery, corresponded to either the symptomatic artery or the artery with greater stenosis in asymptomatic individuals. Clinical information was obtained through chart review. The procedures and consent forms of our HIPPA-compliant study were reviewed and approved by the institutional review board before study initiation.

MRI Protocol

MR scans were performed using a 3.0 T whole-body scanner (Signa Excite, General Electric Medical Systems) with a dedicated, phased-array, carotid surface coil.²² A standardized protocol²³ adapted for imaging at 3.0 T²⁴ was used to obtain 5 contrast-weighted sequences of carotid arteries in the transverse plane: T1W, CE-T1W, PD, T2W, and TOF. All scans were centered at the bifurcation of the index artery. Flow suppression for black-blood T1W images was achieved with quadruple inversion recovery (QIR),⁷ whereas black-blood T2W and PD images were acquired with a multislice double-inversion recovery sequence.⁸ Gadodiamide (Omniscan, GE Healthcare, United States) was injected intravenously at a dose of 0.1 mmol/kg and a rate of 1 mL/s 5 minutes prior to CE-T1W image acquisition. Scan parameters for each sequence are detailed in Table 1.

Image Review

Three separate reviews of the imaging data were conducted. Each review contained one of 3 combinations of contrast weightings (CW): (1) 2CW: T1W and CE-T1W; (2) 3CW: T1W, CE-T1W, and TOF; or (3) 5CW: T1W, CE-T1W, TOF, PD, and T2W. Two trained reviewers, blinded to clinical information and results from each of the other rounds of review, interpreted each set of images by consensus opinion. 2CW was interpreted first, followed by 3CW after an interval of 1 month from the completion of 2CW, followed by 5CW after an interval of 1 month from the completion of 3CW (Fig. 1). The combination of T1W and CE-T1W was selected during the initial round of review because of the reported ability of T1W to have the highest interscan reproducibility among black-blood techniques,²⁵ and the improvement of LRNC detection using CE-T1W.^{19,20} In the second round of review, a TOF weighting was added based on its reported usefulness to identify fibrous cap rupture¹⁵ and its role in detecting IPH.^{2,13} In the third round of review, T2W and PD were added according to the utilization of a shared echo technique (double-echo imaging) for the acquisition of these sequences (Table 1). During each round of review, image quality (ImQ) was rated per slice for each artery using a 4-point scale (1 = poor, 4 = excellent²⁶). For images with ImQ >1, image analysis software²⁷ was used to draw the lumen and outer wall boundaries at each axial location. Lumen volume, wall volume, total vessel volume, and mean wall thickness were recorded for each artery. In addition, the presence or absence of

calcification, LRNC, and IPH, and the status of the fibrous cap were identified. Volume measurements of calcification, LRNC, and IPH, when present, were also collected.

Data Analysis

Arterial characteristics and prevalence of calcification, LRNC, IPH, and fibrous cap rupture are reported based on results from the 5CW image review. The intraclass correlation coefficient (ICC) and its 95% confidence interval were calculated to assess agreement for morphologic component measurements between 2CW and 3CW compared with 5CW. Calculation of ICCs for component measurements was limited to only cases where the feature was present at both data points. Cohen's kappa (κ) was used to evaluate agreement for the identification of plaque components and surface disruption by 2CW and 3CW compared with 5CW. In accordance with Oppo et al,²⁸ the following criteria for clinically relevant agreement were used: fair, κ value of <0.40; moderate, κ value of 0.40 to 0.60; substantial, κ value of 0.60 to 0.80; and excellent, κ value of >0.80. Strength of classification for identifying the presence or absence of carotid plaque features for 2CW and 3CW compared with 5CW was determined by area-under-the-curve (AUC) from receiver operating characteristics (ROC) analysis. Statistical analysis was performed using SPSS 12.0 for Windows (SPSS Inc, Chicago, IL). Statistical significance was defined as a value of $P < 0.05$.

RESULTS

From October 2005 to December 2007, 67 participants (N = 30 symptomatic, N = 37 asymptomatic) underwent carotid MRI. Of the 67 index arteries evaluated with carotid MRI, 2 (3%) were excluded because of occlusion of the internal carotid artery. Of the remaining 65 carotids, all had sufficient ImQ for quantitative plaque interpretation. Demographic information and carotid plaque characteristics (based on interpretation of 5CW) for this subset (N = 65) are reported in Table 2.

Comparison Between 2CW and 5CW

Across all morphologic measurements, ICC values ranged from 0.95 to 0.99 (Table 3). Agreement for identification of plaque features (Fig. 2) was moderate for calcification ($\kappa = 0.42$; 0.14–0.70) and LRNC ($\kappa = 0.47$; 0.03–0.91), excellent for IPH ($\kappa = 0.88$; 0.76–0.99), and fair for surface disruption ($\kappa = 0.34$; 0.14–0.54). 2CW was able to detect 92.3% of calcification, 98.3% of LRNC, 90% of IPH, and 29.2% of surface disruption identified by 5CW. When calcification, LRNC, or IPH was detected on both 2CW and 5CW, agreement between volume measurements (Table 3) was strongest for LRNC (ICC = 0.98), followed by IPH (ICC = 0.90) and calcification (ICC = 0.89). Of note, a 2CW acquisition would reduce scan time by approximately 7 minutes (29.1%) compared with the 5CW acquisition assuming a dual-echo acquisition for PD and T2W (Table 1).

Comparison Between 3CW and 5CW

The addition of TOF did not substantially alter the agreement of morphologic measurements with 5CW. ICC values ranged from 0.97 to 1.00 (Table 3). For identification of plaque features (Fig. 2), agreement between 3CW and 5CW was moderate for calcification ($\kappa =$

0.59; 0.34–0.85), substantial for LRNC ($\kappa = 0.75$; 0.47–1.00) and surface disruption ($\kappa = 0.76$; 0.60–0.93), and excellent for IPH ($\kappa = 0.91$; 0.81–1.00). 3CW was able to detect 94.2% of calcification, 95% of LRNC, 96.7% of IPH, and 79.2% of surface disruption identified by 5CW. For volume measurements of plaque components when the component was detected on both 3CW and 5CW, agreement (Table 3) was strongest for LRNC (ICC = 0.97) and IPH (ICC = 0.97) followed by calcification (ICC = 0.83). Of note, a 3CW acquisition would reduce scan time by approximately 4 minutes (16.7%) compared with the 5CW acquisition assuming a dual-echo acquisition for PD and T2W (Table 1).

ROC Analysis

Using 5CW as the reference standard, ROC analysis revealed that 3CW showed larger AUCs than that of 2CW in classifying calcification (0.78 vs. 0.69, respectively), LRNC (0.98 vs. 0.69, respectively), and surface disruption (0.87 vs. 0.65, respectively). Both 2CW (AUC = 0.94) and 3CW (AUC = 0.96) were strong classifiers of carotid IPH.

DISCUSSION

This study reports evidence that comprehensive, quantitative carotid plaque interpretation can be performed with T1W, CE-T1W, and TOF sequences. Elimination of PD and T2W sequences from the carotid MRI protocol may result in a substantial reduction in scan time. In addition, our findings highlight the potential feasibility of further reducing scan time via protocol customization to optimally address specific research or clinical objectives. The ability to perform plaque interpretation on images acquired within a clinically acceptable scan time may broaden the research utility of carotid MRI and increase translatability to clinical applications.

Evaluation of plaque morphology across different CWs has been previously considered. In 2001, Zhang et al found that each black-blood sequence (T1W, PD, and T2W) separately yielded similar measurements of the arterial wall and lumen.²⁹ Because each round of review during our study contained T1W images, the strong agreement in morphology measurements was expected. However, extrapolation of our findings to future studies should be considered within the context of 2 potential confounders: (1) the effects of contrast-enhanced MRI; and (2) surface calcification. Administration of gadolinium-based contrast agents has been shown to significantly alter measures of plaque morphology—decreased lumen size and increased wall size.³⁰ Of note, the effects of lumen size in this previous study³⁰ were observed despite the application of improved T1-insensitive flow suppression techniques.³¹ As such, evaluation of plaque morphology on black-blood MRI should be limited to sequences prior to contrast administration. With regards to surface calcification, the hypointense signal of calcification inhibits differentiation from the true luminal boundary on black-blood MRI (Fig. 3). Our observation that the addition of TOF to T1W and CE-T1W did not substantially alter correspondence with the full imaging protocol may have resulted from a low prevalence and/or small size of surface calcification in this particular cohort. Nevertheless, bright blood sequences, such as TOF, are necessary to accurately characterize the luminal boundary.¹ In accord, evaluating populations with a high-prevalence of carotid calcification (eg, patients with a history of coronary artery disease²⁶) may warrant

the inclusion of a bright-blood sequence in the imaging protocol to optimize quantification of plaque morphology.

Beyond luminal calcification, TOF had a demonstrable benefit in the analysis of fibrous cap rupture (Fig. 4). Identification of fibrous cap rupture is critical because cross-sectional^{16,32} and prospective³³ studies have identified an association between fibrous cap status and ischemic events. Interestingly, the addition of TOF had only a marginal benefit in improvement of IPH detection. At 1.5 T, a hyperintense signal on TOF is the principle criterion for distinguishing IPH within the 5CW imaging protocol. A recent study of IPH detection at 3.0 T using histology as the reference standard, however, found that the black-blood, QIR, T1W sequence performed similar or better than TOF for detection of IPH at 3.0 T.³⁴ Whereas both sequences are T1W, the increase in T1 time observed at higher field-strengths^{35,36} may play favorably toward IPH detection by the black-blood, QIR, T1W sequence.

In the absence of CE-T1W, T2W has been previously used for evaluating the LRNC.^{2,4,37} However, CE-T1W imaging has been shown to (1) afford a higher correlation of quantitative measures compared with histology than T2W¹⁹; and (2) substantially improve reproducibility of measures associated with the LRNC compared with T2W.²⁰ Evidence from prospective studies indicates that size of the LRNC is predictive of both future neurologic events³³ and development of new fibrous cap ruptures.³⁸ Accordingly, accurate and reproducible quantitative assessment of the LRNC is necessary to correctly assess atherosclerotic disease severity and for following disease evolution. Although the benefits of utilizing CE-MRI for evaluation of the LRNC are evident, the association between gadolinium-based contrast agents and nephrogenic systemic fibrosis (NSF) warrants discussion. NSF has emerged as a clinical syndrome linked to gadolinium-based contrast agents in patients with renal insufficiency.^{39,40} As such, acquisition of CE-T1W images for carotid plaque evaluation, particularly in research, should be limited to participants with normal renal function (GFR >60).⁴¹ In addition, there is strong evidence that indicates risk of NSF varies depending with agent.^{42,43} Selection of safer gadolinium-based contrast agents (eg, gadoteridol [ProHance, Bracco Diagnostics]) may further reduce risk of NSF during future investigations. Notably, no patients during our investigation developed NSF.

The unique information that T2W and PD sequences yield in plaque analysis has been determining acuity of IPH.¹³ However, Takaya et al found in a prospective study of IPH that signal intensity on T2W and PD remained constant over a period of 18 months.¹⁴ Their finding suggested that either a continual leakage of red blood cells into the lesion occurred and/or hemorrhage ages differently in the atherosclerotic lesion compared with hemorrhage in the brain.¹³ Consequently, the age of IPH may have limited implications. In addition, the cross-sectional and prospective studies linking IPH with neurologic symptoms have been premised on the presence or absence of IPH, not the age of IPH.

Carotid plaque imaging at 3.0 T has enabled a substantial improvement of signal-to-noise ratio compared with 1.5 T.²³ This increased performance has been used to halve scan time via fewer excitations without compromise of plaque interpretation.²⁴ Removal of T2W and PD from a standardized protocol may further reduce scan time, particularly when T2W and

PD are not acquired with a shared echo technique as has been previously described.^{24,44} In a 3 contrast protocol (T1W, CE-T1W, and TOF), scan time may be better used by exploiting the interval (5 minutes) between contrast administration and acquisition of the postcontrast T1W images. Potential strategies may consider replacement of TOF with a very high spatial resolution CE-MRA.⁴⁵ Although this would require validation of CE-MRA to detect fibrous cap rupture before doing so, this approach would further reduce scan time by 3 to 4 minutes. In so doing, feature specific sequences may be implemented in place of TOF without additional scan time compared with the 3CW combination discussed herein. A technique of 3-dimensional inversion-recovery-based T1W (magnetization-prepared rapid acquisition with gradient-echo) has been used to detect IPH in carotid arteries.⁴⁶ Bitar et al reported 3-dimensional T1W fat-suppressed spoiled gradient-echo sequence showed strong agreement with histology in detecting carotid IPH.⁴⁷ These techniques may provide another option for the CW combination, particularly for IPH detection.

We conclude that the combination of T1W, CE-T1W, and TOF imaging was an effective protocol for comprehensively evaluating carotid atherosclerotic disease. Strategies for reducing scan time without compromising performance may facilitate the application of carotid MRI in clinical practice.

Acknowledgments

Supported by the GE Healthcare and the NIH grant (RO1 HL 56874).

References

1. Mitsumori LM, Hatsukami TS, Ferguson MS, et al. In vivo accuracy of multisequence MR imaging for identifying unstable fibrous caps in advanced human carotid plaques. *J Magn Reson Imaging*. 2003; 17:410–420. [PubMed: 12655579]
2. Yuan C, Mitsumori LM, Ferguson MS, et al. In vivo accuracy of multispectral magnetic resonance imaging for identifying lipid-rich necrotic cores and intraplaque hemorrhage in advanced human carotid plaques. *Circulation*. 2001; 104:2051–2056. [PubMed: 11673345]
3. Saam T, Ferguson MS, Yarnykh VL, et al. Quantitative evaluation of carotid plaque composition by in vivo MRI. *Arterioscler Thromb Vasc Biol*. 2005; 25:234–239. [PubMed: 15528475]
4. Trivedi RA, U-King-Im J, Graves MJ, et al. Multi-sequence in vivo MRI can quantify fibrous cap and lipid core components in human carotid atherosclerotic plaques. *Eur J Vasc Endovasc Surg*. 2004; 28:207–213. [PubMed: 15234703]
5. Puppini G, Furlan F, Cirotta N, et al. Characterisation of carotid atherosclerotic plaque: comparison between magnetic resonance imaging and histology. *Radiol Med*. 2006; 111:921–930. [PubMed: 17021689]
6. Clarke SE, Hammond RR, Mitchell JR, et al. Quantitative assessment of carotid plaque composition using multicontrast MRI and registered histology. *Magn Reson Med*. 2003; 50:1199–1208. [PubMed: 14648567]
7. Yarnykh VL, Yuan C. T1-insensitive flow suppression using quadruple inversion-recovery. *Magn Reson Med*. 2002; 48:899–905. [PubMed: 12418006]
8. Yarnykh VL, Yuan C. Multislice double inversion-recovery black-blood imaging with simultaneous slice reinversion. *J Magn Reson Imaging*. 2003; 17:478–483. [PubMed: 12655588]
9. Yuan C, Beach KW, Smith LH Jr, et al. Measurement of atherosclerotic carotid plaque size in vivo using high resolution magnetic resonance imaging. *Circulation*. 1998; 98:2666–2671. [PubMed: 9851951]

10. Zhang S, Suri JS, Salvado O, et al. Inter- and intra-observer variability assessment of in vivo carotid plaque burden quantification using multi-contrast dark blood MR images. *Stud Health Technol Inform.* 2005; 113:384–393. [PubMed: 15923749]
11. Kampschulte A, Ferguson MS, Kerwin WS, et al. Differentiation of intraplaque versus juxtaluminal hemorrhage/thrombus in advanced human carotid atherosclerotic lesions by in vivo magnetic resonance imaging. *Circulation.* 2004; 110:3239–3244. [PubMed: 15533871]
12. Cappendijk VC, Cleutjens KB, Heeneman S, et al. In vivo detection of hemorrhage in human atherosclerotic plaques with magnetic resonance imaging. *J Magn Reson Imaging.* 2004; 20:105–110. [PubMed: 15221815]
13. Chu B, Kampschulte A, Ferguson MS, et al. Hemorrhage in the atherosclerotic carotid plaque: a high-resolution MRI study. *Stroke.* 2004; 35:1079–1084. [PubMed: 15060318]
14. Takaya N, Yuan C, Chu B, et al. Presence of intraplaque hemorrhage stimulates progression of carotid atherosclerotic plaques: a high-resolution magnetic resonance imaging study. *Circulation.* 2005; 111:2768–2775. [PubMed: 15911695]
15. Hatsukami TS, Ross R, Polissar NL, et al. Visualization of fibrous cap thickness and rupture in human atherosclerotic carotid plaque in vivo with high-resolution magnetic resonance imaging. *Circulation.* 2000; 102:959–964. [PubMed: 10961958]
16. Yuan C, Zhang SX, Polissar NL, et al. Identification of fibrous cap rupture with magnetic resonance imaging is highly associated with recent transient ischemic attack or stroke. *Circulation.* 2002; 105:181–185. [PubMed: 11790698]
17. Winn WB, Schmiedl UP, Reichenbach DD, et al. Detection and characterization of atherosclerotic fibrous caps with T2-weighted MR. *Am J Neuroradiol.* 1998; 19:129–134. [PubMed: 9432170]
18. Wasserman BA, Smith WI, Trout HH III, et al. Carotid artery atherosclerosis: in vivo morphologic characterization with gadolinium-enhanced double-oblique MR imaging initial results. *Radiology.* 2002; 223:566–573. [PubMed: 11997569]
19. Cai J, Hatsukami TS, Ferguson MS, et al. In vivo quantitative measurement of intact fibrous cap and lipid-rich necrotic core size in atherosclerotic carotid plaque: comparison of high-resolution, contrast-enhanced magnetic resonance imaging and histology. *Circulation.* 2005; 112:3437–3444. [PubMed: 16301346]
20. Takaya N, Cai J, Ferguson MS, et al. Intra- and inter-reader reproducibility of magnetic resonance imaging for quantifying the lipid-rich necrotic core is improved with gadolinium contrast enhancement. *J Magn Reson Imaging.* 2006; 24:203–210. [PubMed: 16739123]
21. Yuan C, Kerwin WS, Yarnykh VL, et al. MRI of atherosclerosis in clinical trials. *NMR Biomed.* 2006; 19:636–654. [PubMed: 16986119]
22. Hayes CE, Mathis CM, Yuan C. Surface coil phased arrays for high-resolution imaging of the carotid arteries. *J Magn Reson Imaging.* 1996; 6:109–112. [PubMed: 8851414]
23. Yarnykh VL, Terashima M, Hayes CE, et al. Multicontrast black-blood MRI of carotid arteries: comparison between 1.5 and 3 tesla magnetic field strengths. *J Magn Reson Imaging.* 2006; 23:691–698. [PubMed: 16555259]
24. Underhill HR, Yarnykh VL, Hatsukami TS, et al. Carotid plaque morphology and composition: initial comparison between 1.5- and 3.0-T magnetic field strengths. *Radiology.* 2008; 248:550–560. [PubMed: 18574135]
25. Kang X, Polissar NL, Han C, et al. Analysis of the measurement precision of arterial lumen and wall areas using high-resolution MRI. *Magn Reson Med.* 2000; 44:968–972. [PubMed: 11108636]
26. Underhill HR, Yuan C, Terry JG, et al. Differences in carotid arterial morphology and composition between individuals with and without obstructive coronary artery disease: a cardiovascular magnetic resonance study. *J Cardiovasc Magn Reson.* 2008; 10:31. [PubMed: 18549502]
27. Kerwin W, Xu D, Liu F, et al. Magnetic resonance imaging of carotid atherosclerosis: plaque analysis. *Top Magn Reson Imaging.* 2007; 18:371–378. [PubMed: 18025991]
28. Oppo K, Leen E, Angerson WJ, et al. Doppler perfusion index: an interobserver and intraobserver reproducibility study. *Radiology.* 1998; 208:453–457. [PubMed: 9680575]
29. Zhang S, Hatsukami TS, Polissar NL, et al. Comparison of carotid vessel wall area measurements using three different contrast-weighted black blood MR imaging techniques. *Magn Reson Imaging.* 2001; 19:795–802. [PubMed: 11551719]

30. Phan BA, Chu B, Kerwin WS, et al. Effect of contrast enhancement on the measurement of carotid arterial lumen and wall volume using MRI. *J Magn Reson Imaging*. 2006; 23:481–485. [PubMed: 16523478]
31. Yarnykh VL, Yuan C. Simultaneous outer volume and blood suppression by quadruple inversion-recovery. *Magn Reson Med*. 2006; 55:1083–1092. [PubMed: 16598725]
32. Saam T, Cai J, Ma L, et al. Comparison of symptomatic and asymptomatic atherosclerotic carotid plaque features with in vivo MR imaging. *Radiology*. 2006; 240:464–472. [PubMed: 16864672]
33. Takaya N, Yuan C, Chu B, et al. Association between carotid plaque characteristics and subsequent ischemic cerebrovascular events: a prospective assessment with MRI—initial results. *Stroke*. 2006; 37:818–823. [PubMed: 16469957]
34. Ota H, Yarnykh VL, Ferguson MS, et al. Carotid intraplaque hemorrhage imaging at 3.0-tesla MRI: a comparison of the diagnostic performance of three T1-weighted sequences. *Radiology*. In press.
35. de Bazelaire CM, Duhamel GD, Rofsky NM, et al. MR imaging relaxation times of abdominal and pelvic tissues measured in vivo at 3.0 T: preliminary results. *Radiology*. 2004; 230:652–659. [PubMed: 14990831]
36. Gold GE, Han E, Stainsby J, et al. Musculoskeletal MRI at 3.0 T: relaxation times and image contrast. *Am J Roentgenol*. 2004; 183:343–351. [PubMed: 15269023]
37. Cai JM, Hatsukami TS, Ferguson MS, et al. Classification of human carotid atherosclerotic lesions with in vivo multicontrast magnetic resonance imaging. *Circulation*. 2002; 106:1368–1373. [PubMed: 12221054]
38. Underhill HR, Yuan C, Yarnykh VL, et al. Predictors of surface disruption with MR imaging in asymptomatic carotid artery stenosis. *Am J Neuroradiol*. Epub ahead of print.
39. Grobner T. Gadolinium—a specific trigger for the development of nephrogenic fibrosing dermopathy and nephrogenic systemic fibrosis? *Nephrol Dial Transplant*. 2006; 21:1104–1108. [PubMed: 16431890]
40. Rydahl C, Thomsen HS, Marckmann P. High prevalence of nephrogenic systemic fibrosis in chronic renal failure patients exposed to gadodiamide, a gadolinium-containing magnetic resonance contrast agent. *Invest Radiol*. 2008; 43:141–144. [PubMed: 18197066]
41. Sadowski EA, Bennett LK, Chan MR, et al. Nephrogenic systemic fibrosis: risk factors and incidence estimation. *Radiology*. 2007; 243:148–157. [PubMed: 17267695]
42. Wiginton CD, Kelly B, Oto A, et al. Gadolinium-based contrast exposure, nephrogenic systemic fibrosis, and gadolinium detection in tissue. *Am J Roentgenol*. 2008; 190:1060–1068. [PubMed: 18356456]
43. Varani J, DaSilva M, Warner RL, et al. Effects of gadolinium-based magnetic resonance imaging contrast agents on human skin in organ culture and human skin fibroblasts. *Invest Radiol*. 2009; 44:74–81. [PubMed: 19077912]
44. Saam T, Hatsukami TS, Yarnykh VL, et al. Reader and platform reproducibility for quantitative assessment of carotid atherosclerotic plaque using 1.5T Siemens, Philips, and General Electric scanners. *J Magn Reson Imaging*. 2007; 26:344–352. [PubMed: 17610283]
45. DeLano MC, DeMarco JK. 3.0 T versus 1.5 T MR angiography of the head and neck. *Neuroimaging Clin N Am*. 2006; 16:321–341. xi. [PubMed: 16731370]
46. Yamada N, Higashi M, Otsubo R, et al. Association between signal hyper-intensity on T1-weighted MR imaging of carotid plaques and ipsilateral ischemic events. *Am J Neuroradiol*. 2007; 28:287–292. [PubMed: 17296997]
47. Bitar R, Moody AR, Leung G, et al. In vivo 3D high-spatial-resolution MR imaging of intraplaque hemorrhage. *Radiology*. 2008; 249:259–267. [PubMed: 18796681]

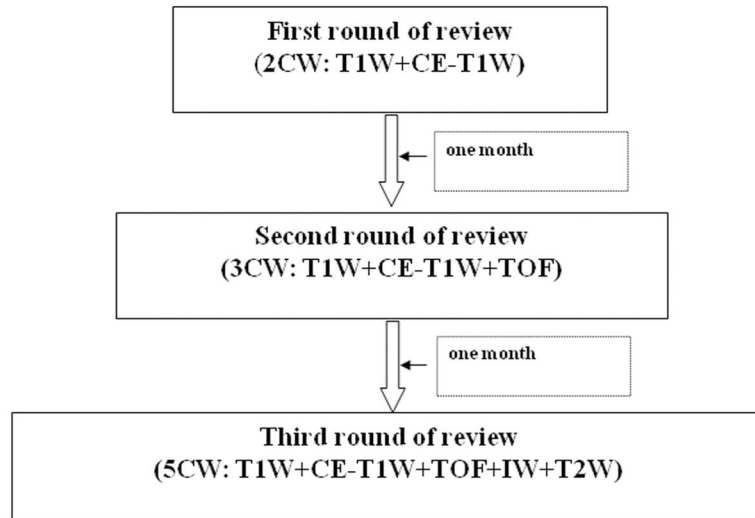


FIGURE 1.
A flow chart of image review.

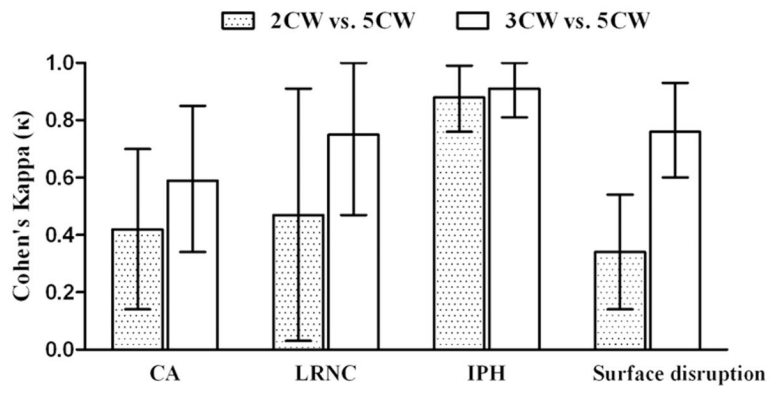


FIGURE 2. Agreement for identification of plaque features between each round of review. The error bar represents 95% confidence interval for κ . CA indicates calcification; LRNC, lipid-rich necrotic core; IPH, intraplaque hemorrhage.

Author Manuscript

Author Manuscript

Author Manuscript

Author Manuscript

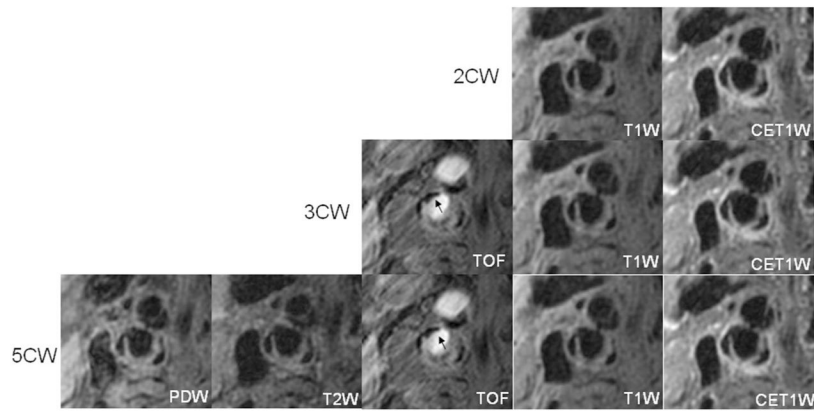


FIGURE 3. Images are from the right internal carotid artery of a 90-year-old male patient with neurologic symptoms. Without addition of TOF, the surface calcification (arrow) seems to be part of the lumen on T1W and CE-T1W (2CW).

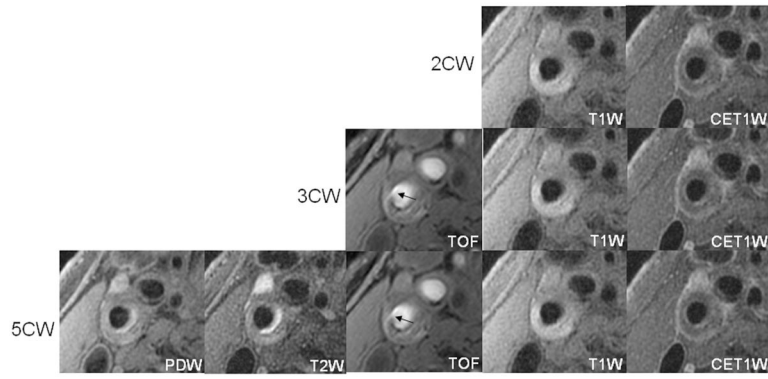


FIGURE 4.

Images are from the right internal carotid artery of an asymptomatic 62-year-old male patient. A fibrous cap rupture was detected after the addition of TOF to the black blood contrast weightings (2CW) because of the presence of jux-taluminal hemorrhage (arrow). No evidence of fibrous cap rupture was found on black blood images alone.

TABLE 1

Carotid Imaging Parameters

Parameters	Black-Blood PD	Black-Blood T2W	Black-Blood T1W	TOF MRA
Contrast	No	No	No/yes	No
Sequence *	FSE	FSE	FSE	SPGR
Image mode	2D	2D	2D	3D
Scan plane	Axial	Axial	Axial	Axial
TR, msec	3000	3000	800	29
TE, msec	10–13.1	60–66	8.8	2.1
FOV, cm	14 × 14	14 × 14	14 × 14	14 × 14
Matrix size	256 × 256	256 × 256	256 × 256	256 × 256
Resolution, mm ²	0.55 × 0.55	0.55 × 0.55	0.55 × 0.55	0.55 × 0.55
Slice thickness, mm	2	2	2	2
No. slices	12	12	12	24
Blood suppression †	MDIR	MDIR	QIR	Saturation–veins
No. excitations	2	2	2	1
Special parameters	Echo train 12; 8 slices/TR	Echo train 12; 8 slices/TR	Echo train 8	Flip angle 20 degree
Fat suppression	Yes	Yes	Yes	No
Scan time, min		4‡	6/5/6§	3

* GE acronyms.

† Special blood-suppression techniques MDIR and QIR are performed with custom-designed software.

‡ PD and T2W sequences were acquired using a shared echo technique (double-echo imaging).

§ The scan time of black-blood T1W corresponds to precontrast acquisition/delay/postcontrast acquisition.

TABLE 2

The Characteristics of the Study Population

Characteristic and Risk Factor	Mean \pm SD or %	Range
Age (yr)	66.7 \pm 11.6	30–90
Gender	56 men, 9 women	—
Height (m)	1.7 \pm 0.1	1.5–1.8
Weight (kg)	69.4 \pm 10	50–90
Body mass index (kg/m ²)	24.1 \pm 3.0	18.0–30.9
Hypertension	67.7%	—
Antihypertensive drugs	66.2%	—
Smoker	41.5%	—
Diabetes mellitus	15.4%	—
History of coronary artery disease	32.3%	—
Neurological symptoms	41.5%	—
Lumen volume (mm ³)	657.7 \pm 273.4	240.7–1512.6
Wall volume (mm ³)	928.4 \pm 468.0	354.0–3444.1
Total vessel volume (mm ³)	1586.1 \pm 637.5	648.9–4956.7
Mean wall thickness (mm)	1.9 \pm 0.6	0.8–3.7
Presence of LRNC	92.3%	—
Presence of IPH	46.2%	—
Presence of CA	80%	—
Presence of fibrous cap rupture	36.9%	—
Volume of LRNC (mm ³) [*]	302.1 \pm 340.6	21.0–2164.7
Volume of IPH (mm ³) [*]	159.8 \pm 196.6	1.6–941.9
Volume of CA (mm ³) [*]	47.2 \pm 48.1	0.9–176.5

* In arteries with feature present.

TABLE 3

Intraclass Correlation Coefficients for Plaque Morphology and Components

MR Measurements	N	2CW Versus 5CW		3CW Versus 5CW	
		ICC	95% CI	ICC	95% CI
Lumen volume	65	0.98	0.97–0.99	0.99	0.99–1.00
Wall volume	65	0.98	0.97–0.99	0.99	0.98–0.99
Total vessel volume	65	0.99	0.99–1.00	1.00	0.99–1.00
Mean wall thickness	65	0.95	0.92–0.97	0.97	0.95–0.98
Calcification volume	47	0.89	0.80–0.94	0.83	0.77–0.90
LRNC volume	57	0.98	0.97–1.0	0.97	0.96–0.99
IPH volume	27	0.90	0.79–0.95	0.97	0.94–0.99